The infrared spectrum of He–HCO$^+$

S. A. Nizkorodov, J. P. Maier, and E. J. Bieske
Institut für Physikalische Chemie, Universität Basel, Klingelbergstr. 80, CH-4056 Basel, Switzerland

(Received 28 March 1995; accepted 17 April 1995)

The vibrational predissociation spectrum of the He–HCO$^+$ proton bound complex has been recorded in the 3 μm (C–H stretch) region by monitoring the HCO$^+$ photofragment current. A rotationally resolved, parallel band is observed, red shifted 12.4 cm^{-1} from the ν_1 transition of free HCO$^+$. Analysis in terms of a diatomiclike Hamiltonian yields $B''=0.2900\pm0.0002$ cm^{-1}, $D''=(1.00\pm0.06)\times10^{-5}$ cm^{-1}, $B'=0.2898\pm0.0010$ cm^{-1}, and $\nu_1=3076.313\pm0.010$ cm^{-1}. Localized perturbations to ν_1 rotational levels are observed and are tentatively ascribed to interactions with combination vibrational states made up of quanta of the CO stretch and HCO$^+$ bend, and those of the low frequency intermolecular stretches and bends. Rotational linewidths are laser bandwidth limited suggesting a lower limit of approximately 250 ps for the lifetime of the ν_1 level. © *1995 American Institute of Physics.*

I. INTRODUCTION

Proton exchange is a fundamental chemical event, playing a central role not only in condensed phase chemistry, but also in the more tenuous surroundings of terrestrial and interstellar plasmas. In the latter, a gamut of exothermic protonation reactions proceed without substantial barrier, and are crucial in the synthesis of larger molecules. In order to fully understand the course of these reactions, and in particular to predict product rovibrational states and branching ratios, detailed knowledge of the reaction hypersurface is desirable. To date such information has largely come from theoretical *ab initio* calculations. Recently we have undertaken spectroscopic explorations of several protonated ion-neutral complexes including H_2–HCO$^+$,[1] He–HN$_2^+$,[2] and H_2–HN$_2^+$,[3] species that may be viewed essentially as de-energized protonation reaction intermediates. In the current work we extend these studies and describe infrared spectroscopic studies of the He–HCO$^+$ complex.

Further impetus for high resolution spectroscopic studies of ionic complexes comes from a desire to augment the substantial body of information concerning neutral van der Waals molecules with comparable data for ionic systems. In so doing we hope to provide insights into factors governing structures, energetics, and dynamics. Numerous spectroscopic studies have addressed the structural attributes of He containing van der Waals molecules, including electronic spectroscopy of I_2–He (Ref. 4) and Cl_2–He,[5] and more recently IR spectroscopy of He–HF,[6] He–CO,[7] and He–CO$_2$.[8] A common feature of these neutral complexes is the fragility of the intermolecular bond; in general the binding energies are less than 30 cm^{-1}, with the potential supporting only one or two bound vibrational states, and a few rotational levels. Due to the contribution of charge induced dipole forces, a somewhat stronger bond can be anticipated for the corresponding ionic complexes. For example, N$_2^+$–He has an intermolecular potential with a well depth close to 140 cm^{-1} and which supports a number of free internal rotorlike bending states and several stretching states.[9,10]

The subject of the current work can be thought of as the intermediate in the exothermic $\mathrm{HeH^+ + CO \rightarrow HCO^+ + He}$ ($\Delta H=-99.5$ kcal/mol) reaction.[11] Previous theoretical and experimental studies show that when two closed shell atoms or molecules coalesce with a proton, the resulting complex has a minimum energy structure such that proton can be most effectively shared between the constituents, with the intermolecular binding energy strongly correlated with the difference in proton affinities. Large differences in proton affinities (PA) imply small binding energies and vice versa. Given that the PA of CO (142 kcal/mol) vastly exceeds the one of He (42.5 kcal/mol) (Ref. 11) one would suspect that the (HCO–He)$^+$ complex will consist essentially of a He atom loosely bound to an almost undistorted HCO$^+$ molecular ion. The current study can be regarded as a companion for our earlier work on the isoelectronic He–HN$_2^+$ complex.[2] Given that the long range electrostatic interactions should be identical for the two systems, one might expect a close structural correspondence. Nevertheless, while it transpires that both complexes are linear, the intermolecular bond turns out to be somewhat weaker in He–HCO$^+$ than it is He–HN$_2^+$. As well there are important differences in the coupling between the intermolecular and intramolecular motions, manifested in variations in vibrational predissociation rates, band shifts in the hydrogen stretching vibration and upper state perturbations.

II. EXPERIMENT

Observation of He–HCO$^+$ infrared absorptions is based upon exciting predissociative vibrational levels with a tunable IR light source while monitoring the photofragment ion current. Details of the tandem mass spectrometer have been discussed in earlier papers dealing both with the IR photodissociation spectra of the He–HN$_2^+$ (Ref. 2) and H_2–HCO$^+$ (Ref. 1) complexes, and also with the resonance enhanced photodissociation of complexes in the visible and UV.[12,10] In short, ionic complexes are formed in an ion source consisting of an electron beam crossed pulsed supersonic expansion, which previous experience shows, is capable of producing molecular [e.g., N$_3^+$ (Ref. 13)] and cluster [N$_2^+$–He$_n$ (Ref. 10)] ions with rotational temperatures in the 30–40 K range. To manufacture He–HCO$^+$ complexes, a mixture of He, CO, and H_2 at 6 bar stagnation pressure and 100:1:1 ratio is used. Ions are coaxed from the supersonic plasma through a 1 mm diam skimmer biased at −5 V with respect to the ion source, and are injected through a series of electrostatic lenses into a quadrupole mass filter where primary mass selection of the parent ion (He–HCO$^+$ in this case) takes place. Subsequently the beam is deflected through 90° by a quadrupole bender, and passes into an octopole ion guide where it is subjected to a 10 ns pulse of tunable infrared light. A second quadrupole mass filter is adjusted to transmit HCO$^+$ photofragment ions which are sensed using a Daly scintillation detector coupled to a boxcar integrator.

Light in the 3 μm region with 0.02 cm^{-1} bandwidth is generated using a Nd:YAG pumped optical parametric oscillator system (Continuum Mirage 3000). In order to calibrate the spectrum a fraction of the IR output was directed into an OCS filled optoacoustic cell, with accurate interpolation between the measured optoacoustic lines facilitated by simultaneously recorded etalon fringes. The 8 eV energy of the ions in the octopole ion guide necessitates a Doppler correction of +0.072 cm^{-1} to the measured line wave numbers. Estimated precision of line wave numbers is ±0.007 cm^{-1}.

Although the mass selective nature of our experiment provides a good deal of confidence that we are in fact observing transitions of the He–HCO$^+$ cation complex, it does not exclude the possibility that complexes containing the less stable isoformyl cation (He–HOC$^+$) are also present. Although the formyl cation HCO$^+$ is believed to be the dominant molecular cation component of dense H_2/CO plasmas, the isomeric isoformyl HOC$^+$ cation is also produced in the primary reaction of H_3^+ with CO.[14] However, as HOC$^+$ is readily converted into the more stable HCO$^+$ by reactions with either CO or H_2,[15] and as the number densities of H_2 and CO in the supersonic plasma are relatively high, it is almost certain that the more stable HCO$^+$ ion (and complexes containing it) will be almost exclusively produced. Nevertheless we searched for IR predissociation signals of the mass 33 ion near both the HOC$^+$ and HCO$^+$ ν_1 band origins (~3268 cm^{-1} and 3089 cm^{-1}, respectively).

III. RESULTS AND ANALYSIS

The vibrational predissociation spectrum of HCO$^+$–He in the 3060–3100 cm^{-1} range is displayed in Fig. 1. As the band is red shifted from the free HCO$^+$ ν_1 origin by only 12.4 cm^{-1} and because thorough searches in the 2950–3290 cm^{-1} span failed to reveal other transitions, we feel justified in presuming that the illustrated band indeed arises from excitation of the He–HCO$^+$ ν_1 C–H stretch vibration. The signal to noise ratio in the spectrum is somewhat worse than it was for the corresponding band of He–HN$_2^+$ recorded under similar experimental conditions,[2] reflecting both a lower He–HCO$^+$ parent ion current, and probably also the factor of 3 lower transition intensity of the ν_1 mode in HCO$^+$ compared to HN$_2^+$.[16]

While at first glance the spectrum shown in Fig. 1 appears to possess the ordered structure anticipated for a linear molecule Σ–Σ transition, closer inspection reveals deviations from regular line spacings in both P and R branches, often with the concurrent presence of additional lines, indicating that upper state rotational manifold is beset by perturbations. In the absence of prior ground state information, the presence of the perturbations make spectral assignment somewhat troublesome, especially for the higher J levels. Assignments were accomplished, and ground state inertial and distortion rotational constants were obtained by forming the combination differences,

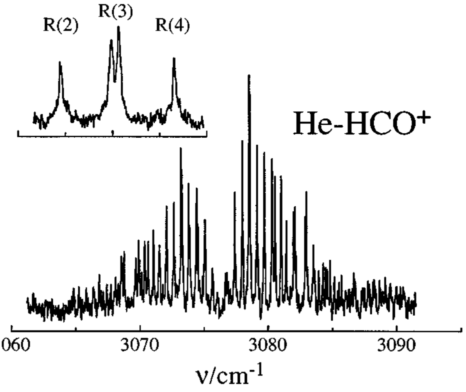

FIG. 1. Vibrational predissociation spectrum of the C–H stretch band (ν_1 vibration) of the He–HCO$^+$ proton bound complex. The spectrum was obtained by monitoring the HCO$^+$ photofragment current as the infrared laser wavelength was scanned. Although the spectrum has roughly the structure expected for a linear molecule Σ–Σ transition, there are irregularities caused by upper state perturbations. Assigned line positions are given in Table I. The inset shows splitting in the $R(3)$ line due to perturbation of $J'=4$.

$$\begin{aligned}\Delta_2F'(J)&=R(J-1)-P(J+1)\\&=2B''(2J+1)-4D''(2J^3+3J^2+3J+1)\end{aligned}\tag{1}$$

between lines with a presumed common upper state in the P and R branches. Line assignments were performed progressively with increasing J, improved values of B'' and D'' at each J being used to predict combination differences for higher levels. Final assignments along with the measured line positions (averaged from four separate spectra) are given in Table I. Ground state B'' and D'' values are, respectively, 0.2900±0.0002 cm^{-1} and (1.00±0.06)×10^{-5} cm^{-1}. Confidence in the extracted constants and assignments is engendered by the fact that in all cases the difference between the measured and calculated combination differences are less than 0.01 cm^{-1} (laser bandwidth ≈0.02 cm^{-1}). As well, virtually all of the observed lines are accounted for in the scheme. Alternative numberings resulted in ground state constants that were appreciably less well determined and more unassigned lines.

While extraction of accurate upper state constants is complicated by perturbations, rough values can be obtained by fitting the positions of the lines that do not suffer obvious large shifts (i.e., excluding lines involving $J'=4$, 8, and $\geqslant 9$) to the familiar expression

$$\begin{aligned}\nu=\nu_0&+(B'+B'')m+(B'-B''-D'+D'')m^2\\&-2(D'+D'')m^3-(D'-D'')m^4\end{aligned}\tag{2}$$

with $m=-J$ for the P branch and $J+1$ for the R branch. For the fit, B'' and D'' were constrained to the values determined

TABLE I. Assigned rotational line wave numbers (cm^{-1}) for P and R branches of the ν_1 band of He–HCO$^+$. Due to perturbations, an extra line appears at certain J values. Differences ($\times 10^{-3}$ cm^{-1}) between the measured line positions and those calculated using the constants given in Table II are listed in the last column.

J''	$P(J'')$ (cm^{-1})	meas−calc ($\times 10^{-3}$ cm^{-1})	J''	$R(J'')$ (cm^{-1})	meas−calc ($\times 10^{-3}$ cm^{-1})
1	3075.733	0			
2	75.150	−3	0	3076.899	6
3	74.578	6	1	77.476	5
4	73.991	−1	2	78.044	−5
5	73.456	44	3	78.663	38
5	73.389	−23	3	78.597	−28
6	72.826	−8	4	79.199	−1
7	72.247	−8	5	79.764	−10
8	71.688	10	6	80.354	9
9	71.226	123	7	81.044	130
9	70.767	−336	7	80.582	−332
10	70.496	−33	8	81.446	−35
11	70.005	48	9	82.092	47
12	69.766	379	10	82.978	372
12	68.773	−614	10	81.987	−619
13	68.541	−279	11	82.899	−265
14	68.069	−186	12	83.527	−192
15	67.710	17	13	84.291	21
15	67.376	−317	13	83.947	−323
16	66.788	−345	14	84.472	−345

from the combination difference analysis, and D' was fixed equal to D''. The ν_0 and B' values determined in this manner were 3076.313±0.010 cm^{-1} and 0.2898±0.0010 cm^{-1}, respectively. Differences between the measured line positions and those predicted using these molecular constants are given in the final column of Table I and are plotted as a function of J' in Fig. 2. It can be seen that whereas, with the exception of $J'=4$ and 8, the positions of lower J' peaks are predicted reasonably well using the fitted constants, for $J'>10$ substantial excursions from the predicted positions are more or less the rule. Small adjustments to the upper state constants do not greatly help in diminishing deviations between measured and calculated positions.

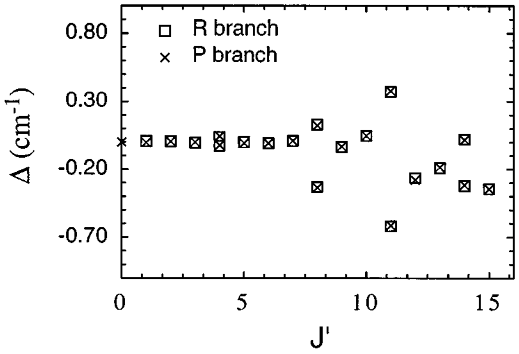

FIG. 2. Differences between measured and calculated (using constants listed in Table II) R and P branch line positions. Note that most points consist of superimposed P and R branch points. The plotted differences are also listed in the last column of Table I.

Slow scans at reduced power (≤200 μJ/pulse) over some of the more intense rotational lines (see the inset to Fig. 1), demonstrate that their widths are laser bandwidth limited (0.02 cm^{-1}), allowing a lower limit of approximately 250 ps to be put on the upper state lifetime. As far as we could ascertain, there does not appear to be any J dependence for the linewidths, although poor S/N ratio for $J>10$ makes accurate measurements for higher J difficult. The deduced upper state lifetime is somewhat longer than for the ν_1 band of He–HN$_2^+$ where corresponding measurement yielded a lifetime of ≈50 ps.[2]

IV. DISCUSSION

A. General

The He–HCO$^+$ complex belongs to a broad class of proton-bound AHB$^+$ species. Although detailed spectroscopic information on these complexes is only beginning to emerge, a series of thermochemical measurements shows that in general their cohesion is inversely related to the difference in the proton affinities of A and B.[17] Thus a large disparity in PA can be associated with a complex where the proton is primarily attached to the higher PA moiety with the other partner bound mainly by electrostatic and induction forces. On the other hand, a small difference is associated with species characterized by reasonably strong intermolecular bonds. Recent spectroscopic work on related complexes [He–HN$_2^+$ (Ref. 2) and H$_2$–HCO$^+$ (Ref. 1)] suggests that although the proton is firmly attached to the constituent with the higher affinity, the other element is arranged so as to maximize its interaction with the proton. Given the relative PA's of CO and He [142 kcal/mol vs 42.5 kcal/mol (Ref. 11)] one anticipates a linear He···HCO$^+$ minimum energy structure for the complex, with the HCO$^+$ properties (bond lengths and vibrational frequencies) left largely intact. These expectations are confirmed by the He–HCO$^+$ infrared spectrum which exhibits a characteristic (albeit perturbed) linear molecule Σ–Σ band, red shifted by 12.4 cm^{-1} from the C–H stretch transition of free HCO$^+$.

Further insight into the nature of the He···HCO$^+$ intermolecular bond can be derived from examination of the ground state rotational and centrifugal distortion constants. Although the present data are not sufficient to precisely determine the equilibrium separation (R_e), if one neglects zero point excursions and assumes an undistorted HCO$^+$ monomer (it is actually likely that the C–H bond will elongate somewhat due to marginal proton transfer to the He atom), a H···He bond distance of 2.00 Å is found. It is worth pointing out that the alternative He···OCH$^+$ structure requires a considerably longer intermolecular bond (He···O distance of around 3.13 Å) to be consistent with the measured rotational constant. Although this is slightly less than the sum of the He and O van der Waals radii (≈3.4 Å), the proton bound form is more consistent with the C–H stretch red shift (≈12.4 cm^{-1}), as it is with the notion that the intermolecular bonding should be dominated by induction interactions between the He and the proton. An assessment of the intermolecular bond strength can be derived by inserting the ground state rotational and centrifugal distortion constants into the expression[18]

$$\omega_s=\sqrt{(4B^3_{\mathrm{complex}}/D_{\mathrm{complex}})[1-(B_{\mathrm{complex}}/B_{\mathrm{HCO^+}})]}.$$

With $B_{\mathrm{HCO^+}}=1.488\ \mathrm{cm}^{-1}$, this yields $\omega_s\approx 90\ \mathrm{cm}^{-1}$ and an harmonic force constant of 1.64 N/m [via the relationship $k=16\pi^2\mu c^2 B^3_{\mathrm{complex}}/D_{\mathrm{complex}}(1-B_{\mathrm{complex}}/B_{\mathrm{HCO^+}})$]. While the spectra do not provide direct information on the intermolecular potential well depth, we remark that the charge induced dipole stabilization energy for a He atom displaced by 2.5 Å from a proton is around $-300\ \mathrm{cm}^{-1}$.

Although the He–HCO$^+$ IR spectrum provides useful impressions of the He$\cdots$HCO$^+$ intermolecular interaction, it is not sufficient to fully define the angular and radial parts of the intermolecular potential. The problems encountered when one seeks to relate the spectroscopically determined B and D values to a purely radial potential are exemplified by studies of the related Ar–HCN van der Waals molecule, which has been characterized in the microwave (pure rotational transitions) and IR [excitation of intermolecular bend[19] and of ν_1 (Refs. 20, 21)]. While Ar–HCN appears to have a linear hydrogen bonded equilibrium geometry, there is little encumberance to the Ar moving around into the T-shaped configuration favored by dispersive interactions with the HCN π^* molecular orbital. Zero point bending excursions are substantial. As the distance between the constituents' centers of mass is much smaller in the T-shaped configuration than it is in the linear one, and as rotation tends to bring the intermolecular bond into alignment with the HCN axis, there is a marked rotational dependence of the effective rotational constant, manifesting itself as an anomalously large centrifugal distortion constant. In fact, extreme angular fluxionality in Ar–HCN was originally diagnosed on the basis of its extraordinarily large centrifugal distortion constant compared to the HF–Ar and HCl–Ar hydrogen bonded dimers, and also by the necessity of including higher order distortion terms to fit the experimental data.[21,22] Subsequently transitions to Σ and Π type bending states, correlating with the HCN $j=1$ rotational state, were located 5.5 cm^{-1} and 6.1 cm^{-1}, respectively above the zero energy level.[19]

As He–HCO$^+$ features a large ground state centrifugal distortion (around 50% larger than in He–HN$_2^+$), and may have an intermolecular potential energy surface permitting facile access to a T-shaped configuration, it is reasonable to wonder whether it also undergoes large amplitude zero point bending displacements. While it is difficult to definitely answer this question without further information on the bending vibrational energy levels (e.g., observation of $\nu_1+\nu_5$), there are several pieces of evidence that suggest that the potential is somewhat stiffer than in the corresponding neutral complexes. First and foremost the appearance of a single Σ–Σ type band with line spacings corresponding to twice the rotational constant of the entire complex, is itself an indication that the complex is more or less effectively ''locked into'' a semirigid linear geometry. If on the other hand, the angular potential was sufficiently isotropic for the complex to be a free internal rotor, the quantum number corresponding to the internal rotation of the HCO$^+$ (j) would be almost good and, assuming that the transition moment for the ν_1 transition remained along the HCO$^+$ axis, the transition would be accompanied by $\Delta j=\pm 1$ changes. Under these circumstances at modest resolution, the spectrum would appear much like the one of a free HCO$^+$ molecule, consisting of P and R branch ''lines'' separated by twice the HCO$^+$ rotational constant ($b\approx 1.487\ \mathrm{cm}^{-1}$). Each of the P and R branch ''lines'' would in fact consist of a series of overlapping $\Delta l=0$ transitions (where l is the quantum number corresponding to end-over-end rotation of the entire complex). For intermediate hindering potentials the spectrum in the ν_1 region should consist of a Σ–Σ type band [corresponding to the nominally forbidden $(\nu_1=1,\ j=0)\leftarrow(\nu_1=0,\ j=0)$ free rotor transition] along with Σ–Σ and Π–Σ type combination bands (both corresponding to the allowed $(\nu_1=1,\ j=1)\leftarrow(\nu_1=1,\ j=0)$ free rotor transition). This intermediate case appears to pertain to the ν_1 transition of Ar–HCN, although the Σ–Σ combination band has not yet been observed.[20,19,21] In addition the apparent absence of bending hot bands in the He–HCO$^+$ spectrum constitutes evidence for a relatively stiff He–HCO$^+$ structure. We estimate that we would observe bending hot band transitions (e.g., $\nu_1+\nu_5-\nu_5$) if the ν_5 state had more than 20% of the ground state population. Assuming a Boltzmann distribution and a vibrational temperature matching the rotational one (30 K) one can estimate that $\nu_5\geqslant 35\ \mathrm{cm}^{-1}$.

B. Perturbations

We consider now the perturbations afflicting some ν_1 rotational levels. A characteristic feature of the perturbations is that for the lower J' values they are localized, principally at $J'=4$ and $J'=8$, while for $J'\geqslant 11$ almost all levels appear to be affected. As the total angular momentum of any two interacting levels must be identical, it is difficult to believe that all perturbing levels are associated with a single vibrational state. Considering the $J'=4$ levels first, we note that the $R(3)$ and $P(5)$ transitions both consist of two lines with similar intensities (Fig. 1) having opposite and roughly equal displacements from the expected energy (Fig. 2), indicating that in the absence of any coupling the interacting pair of $J'=4$ levels would practically coincide (see Fig. 2). Absence of substantial displacement or splitting for the $J'=3$ and 5 levels (Fig. 2) suggests that the interacting manifolds are characterized by somewhat different rotational constants. A simple two level perturbation calculation, assuming that the interaction is roughly independent of J', and exploiting the fact that the neighboring $J'=5$ level is practically unshifted (to within 0.01–0.02 cm^{-1}), can be used to deduce that the perturbing state's rotational constant must differ from the one of the ν_1 level by at least 0.003 cm^{-1}, a difference certainly consistent with the perturbing level possessing quanta of the intermolecular stretch and/or bend vibrations. For the $J'=8$ level a similar line of reasoning based on the fact that the $J'=7$ level is apparently unperturbed to within 0.03 cm^{-1} leads to the conclusion that the rotational constant associated with the perturbing state differs in this case by approximately 0.1 cm^{-1}, again consistent with a state involving intermolecular motion. Rovibrational calculations for the He–N$_2^+$

TABLE II. Constants (in cm^{-1}) for ground state and ν_1 levels of He–HCO$^+$. The B'' and D'' values were obtained by forming combination differences as described in the text [Eq. (1)]. The B' and ν_1 values were determined by fitting minimally perturbed transitions to Eq. (2) with B'' and D'' constrained to the combination difference values and $D'=D''$. Two sigma confidence limits in the last two digits of the constants follow each value in brackets.

	Ground state	ν_1
ν		3076.313(10)
B	0.2900(02)	0.2898(10)
$D/10^{-5}$	1.00(06)	

TABLE III. Properties of the He–HCO$^+$, He–HN$_2^+$, H$_2$–HCO$^+$, and H$_2$–HN$_2^+$ proton bound complexes. The quantity $R=\langle 1/R^2\rangle^{-1/2}$ represents the intermolecular proton-ligand separation, insofar as one can assume an undistorted monomer and neglect the effects of zero point vibrations on the moment of inertia. For He–HCO$^+$ and He–NH$_2^+$ the upper state lifetimes are estimated from rotational line widths. For H$_2$–HCO$^+$ the absence of discernible rotational structure in the C–H stretch band suggests an upper state lifetime of less that 1 ps.

	He–HCO^{+a}	He–NH$_2^{+b}$	H$_2$–HCO^{+c}	H$_2$–HN$_2^{+d}$
ΔPA (kcal/mol)^e	99	76	41	17
k_s (N/m)^e	1.64	4.81	9.68	?
R (Å)	2.00	1.72	1.75	?
τ_{vp} (ps)	>250	≈ 50	<1	?
X–H red shift (cm^{-1})	12.4	75	250	>600

[a] Present work.
[b] Reference 2.
[c] Reference 1.
[d] Reference 3.
[e] Reference 11.

complex show that deposition of one quantum in the intermolecular stretch vibration can decrease the effective rotational constant by this order of magnitude.[9]

The conclusion that the ν_1 band is perturbed by several different vibrational levels raises the question of how such a small molecule can have so many states reasonably strongly coupled to ν_1. One feasible prospect is that the perturbing states are of the type $\nu_2+\nu_3+\nu_s+n\nu_b$, quite probable given that the spacing between ν_1 and $\nu_2+\nu_3$ roughly corresponds to the intermolecular ν_s stretching frequency, estimated from the inertial and centrifugal rotational constants (90 cm^{-1}). For the free HCO$^+$ molecule, in the absence of cross anharmonicity terms, the ν_1 vibration [C–H stretch, 3089 cm^{-1} (Ref. 23)] lies around 80 cm^{-1} above the $\nu_2+\nu_3$ combination [bend+C–O stretch, 3012 cm^{-1} (Refs. 24 and 25)]. Due to its larger average intermolecular separation compared to the ground state, excitation of ν_s should have the effect of significantly decreasing the effective potential anisotropy, perhaps to the point where the bending motion is closer to being a free internal rotor. In this case bending vibrational levels correlating with the $j=0$ and $j=1$ free internal rotor states should lie within a few wave numbers of one another making it quite possible for several reasonably strongly coupled vibrational levels to lie close by ν_1.

It is pertinent to note that the corresponding ν_1 band of He–HN$_2^+$ is apparently unperturbed,[2] presumably reflecting the fact that for HN$_2^+$ the $\nu_2+\nu_3$ combination lies almost 300 cm^{-1} below ν_1 (Ref. 26) so that any near-resonant perturbing state built on $\nu_2+\nu_3$ would need to have considerable energy in the intermolecular motions (perhaps more than the intermolecular dissociation energy) and would necessarily interact with the ν_1 state through the agency of higher order (and therefore presumably weaker) coupling terms.

C. Comparison with related species

Attributes of the He–HCO$^+$, He–HN$_2^+$, H$_2$–HCO$^+$, and H$_2$–HN$_2^+$ proton bound complexes are gathered together in Table III. Information includes band shifts for the C–H or N–H stretch vibrations, estimates for the vibrational predissociation lifetimes based on rotational line broadening, force constants for the intermolecular bonds and intermolecular separations. The relatively fragile nature of the He$\cdots$HCO$^+$ bond is emphasized by comparison of its ground state force constant and bond length with the ones of the other complexes. For example the intermolecular bond in He–HCO$^+$ is approximately 0.3 Å longer than it is in He–HN$_2^+$ while the harmonic force constant is one third as large (1.64 N/m compared to 4.81 N/m, although the effects of possible angular-radial coupling should be kept in mind).

Other more general trends may be apprehended in the data. For example, one notes that smaller differences in the constituents' proton affinities can be correlated with stiffer, shorter intermolecular bonds, more rapid vibrational predissociation and a larger red shift for the C–H or N–H stretch vibrations. Compared to the other proton bound complexes, coupling between the valence and intermolecular vibrations in He–HCO$^+$ is particularly feeble, as evidenced by the comparatively small red shift in the C–H stretch (12.4 cm^{-1}) fundamental and its long ν_1 predissociation lifetime (>250 ps). Interaction between the intermolecular and proton motions is somewhat more effective in He–HN$_2^+$, with a 75 cm^{-1} origin shift and a 50 ps vibrational predissociation lifetime. The coupling is even more pronounced in the H$_2$ containing complexes. In H$_2$–HCO$^+$ the C–H stretch band is shifted by more than 250 cm^{-1} from its free molecule position and predissociation is so rapid that almost all vestiges of rotational structure are obscured. Even more remarkably, in H$_2$–HN$_2^+$ the N–H stretch vibration is shifted by more than 600 cm^{-1} to below 2500 cm^{-1}, taking it beyond the range of our spectrometer.[3]

We remark that while the intermolecular bond in He–HCO$^+$ is relatively long and weak compared to other recently studied proton bound species, it appears to be somewhat sturdier than for *neutral* He containing van der Waals molecules. For example He–HF and He–HCl have dissociation energies of only 7.1 cm^{-1} and 10.1 cm^{-1}, respectively, possess only a few bound rotational levels, and are close to being free internal rotors.[6] It seems that in general the intermolecular bonds in the H$_2$ and He containing proton bound complexes are intermediate between those for neutral rare gas containing van der Waals molecules and strongly hydrogen bonded species {e.g., HCN–HF [k_{int}=23.11 N/m (Ref. 27)]}.

V. SUMMARY AND CONCLUSIONS

In the current work we have utilized sensitive laser and mass spectroscopic means to explore structural properties of the He–HCO^+ complex. Spectra recorded in the C–H stretching region strongly suggest that the complex is linear, a geometrical arrangement permitting the most favourable sharing of the proton between CO and He. One notes that He–HCO^+ has a decidedly longer and weaker intermolecular bond than its isoelectronic cousin He–HN_2^+, and displays a much weaker coupling between intramolecular and intermolecular vibrations, evidenced by the modest ν_1 red shift (12.4 cm^{-1}) and long predissociation lifetime (>250 ps).

Although the current work goes some way in characterizing the He$\cdots$$HCO^+$ radial potential, questions relating to its anisotropic character remain unanswered. Most importantly, because of possible radial-angular coupling there are hazards in attributing rotational and centrifugal distortion constants to purely radial properties of the potential. Spectra of combination bands involving the low frequency intermolecular stretching and bending vibrations would be especially useful in providing data relevant to portions of the PES away from the minimum, and might also help to clarify the nature of the ν_1 band perturbations. In future it may be worthwhile to record spectra of isotopomers (e.g., He–$H^{13}CO^+$) which should feature a different set of perturbations due to small variations in the intramolecular and intermolecular frequencies and rotational constants.

ACKNOWLEDGMENTS

E.J.B. acknowledges the gracious hospitality of Dr. G. T. Fraser and Dr. W. J. Lafferty during the period when the spectral data were being analyzed. Support for this work under the Human Capital and Mobility scheme "Structure and Reactivity of Molecular Ions" BBW Grant No. 93.02060 is acknowledged. This work is part of project No. 20-36153.92 of "Schweizerischer Nationalfonds zur Förderung der wissenschaftlichen Forschung."

[1] E. J. Bieske, S. A. Nizkorodov, F. R. Bennett, and J. P. Maier, J. Chem. Phys. **102**, 5152 (1995).
[2] S. A. Nizkorodov, J. P. Maier, and E. J. Bieske, J. Chem. Phys. **102**, 5570 (1995).
[3] E. J. Bieske, S. A. Nizkorodov, F. R. Bennett, and J. P. Maier, Int. J. Mass Spectrom. Ion Proc. (submitted).
[4] R. E. Smalley, D. H. Levy, and L. Wharton, J. Chem. Phys. **64**, 3266 (1976).
[5] J. I. Cline, D. D. Evard, F. Thommen, and K. C. Janda, J. Chem. Phys. **84**, 1165 (1986).
[6] C. M. Lovejoy and D. J. Nesbitt, J. Chem. Phys. **93**, 5378 (1990).
[7] C. E. Chuaqui, R. J. LeRoy, and A. R. W. McKellar, J. Chem. Phys. **101**, 39 (1994).
[8] M. J. Weida, J. M. Sperhac, D. J. Nesbitt, and J. M. Hutson, J. Chem. Phys. **101**, 8351 (1994).
[9] S. Miller, J. Tennyson, B. Follmeg, P. Rosmus, and H. Werner, J. Chem. Phys. **89**, 2178 (1988).
[10] E. J. Bieske, A. M. Soliva, A. Friedmann, and J. P. Maier, J. Chem. Phys. **96**, 28 (1992).
[11] S. G. Lias, J. E. Bartmess, J. F. Liebman, J. L. Holmes, R. D. Levin, and W. G. Mallard, J. Phys. Chem. Ref. Data **17**, Suppl. 1 (1988).
[12] E. J. Bieske, Faraday Trans. **91**, 1 (1995).
[13] A. Friedmann, A. M. Soliva, S. A. Nizkorodov, E. J. Bieske, and J. P. Maier, J. Phys. Chem. **98**, 8896 (1994).
[14] M. F. Jarrold, M. T. Bowers, D. J. DeFrees, A. D. McLean, and E. Herbst, Astrophys. J. **303**, 392 (1986).
[15] M. J. McEwan, in *Advances in Gas Phase Ion Chemistry*, edited by N. G. Adams and L. M. Babcock (JAI, Greenwich, 1992).
[16] E. R. Keim, M. L. Polak, J. C. Owrutsky, J. V. Coe, and R. J. Saykally, J. Chem. Phys. **93**, 3111 (1990).
[17] R. G. Keesee and A. W. Castleman, Jr., J. Phys. Chem. Ref. Data **15**, 1011 (1986).
[18] D. C. Millen, Can. J. Chem. **63**, 1477 (1985).
[19] S. Drucker, A. L. Cooksy, and W. Klemperer, J. Chem. Phys. **98**, 5158 (1993).
[20] G. T. Fraser and A. S. Pine, J. Chem. Phys. **91**, 3319 (1989).
[21] K. R. Leopold, F. G. T., S. E. Novick, and W. Klemperer, Chem. Rev. **94**, 1807 (1994).
[22] K. R. Leopold, F. G. T., F. J. Lin, D. D. Nelson, and W. Klemperer, J. Chem. Phys. **81**, 4922 (1984).
[23] C. S. Gudeman, M. H. Begemann, J. Pfaff, and R. J. Saykally, J. Chem. Phys. **78**, 5837 (1983).
[24] K. Kawaguchi, C. Yamada, S. Saito, and E. Hirota, J. Chem. Phys. **82**, 1750 (1984).
[25] S. C. Foster and A. R. W. McKellar, J. Chem. Phys. **81**, 3424 (1984).
[26] Y. Kabbadj, T. R. Huet, B. D. Rehfuss, C. M. Gabrys, and T. Oka, J. Mol. Spectrosc. **163**, 180 (1994).
[27] B. A. Wofford, S. G. Lieb, and J. W. Bevan, J. Chem. Phys. **87**, 4478 (1987).